Cell Death and Differentiation (2010) 17, 1003–1010

www.nature.com/cdd

Noninvasive molecular imaging of apoptosis *in vivo* using a modified firefly luciferase substrate, Z-DEVD-aminoluciferin

J Hickson*[,1], S Ackler[1], D Klaubert[2], J Bouska[1], P Ellis[1], K Foster[1], A Oleksijew[1], L Rodriguez[1], S Schlessinger[1], B Wang[1] and D Frost[1]

Apoptosis is a highly regulated process of programmed cell death essential for normal physiology. Dysregulation of apoptosis contributes to the development and progression of various diseases, including cancer, neurodegenerative disorders, and chronic heart failure. Quantitative noninvasive imaging of apoptosis in preclinical models would allow for dynamic longitudinal screening of compounds and facilitates a more rapid determination of therapeutic efficacy. In this study, we report the *in vivo* characterization of Z-DEVD-aminoluciferin, a modified firefly luciferase substrate that in apoptotic cells is cleaved by caspase-3 to liberate aminoluciferin, which can be consumed by luciferase to generate a luminescent signal. In two oncology models, namely SKOV3-luc and MDA-MB-231-luc-LN, at 24, 48, and 72 h after treatment with docetaxel, animals were injected with Z-DEVD-aminoluciferin and bioluminescent images were acquired. Significantly more light was detected at 24 ($P<0.05$), 48 ($P<0.01$), and 72 h ($P<0.01$) in the docetaxel-treated group compared with the vehicle-treated group, with caspase-3 activation at these time points confirmed using immunohistochemistry. Importantly, whereas significant differences between groups were detected as early as 24 h after treatment by molecular imaging, caliper measurements were unable to detect a difference for 4–5 additional days. Taken together, these data show that *in vivo* imaging of apoptosis using Z-DEVD-aminoluciferin could provide a sensitive and rapid method for early detection of drug efficacy, which could potentially be used by numerous therapeutic programs.

Cell Death and Differentiation (2010) **17,** 1003–1010; doi:10.1038/cdd.2009.205; published online 8 January 2010

Apoptosis is a highly regulated process of cell death inherent in all cells in the body and therefore is often referred to as 'cell suicide'. Upon activation, the apoptotic program executes a well-characterized sequence of events by which the cell undergoes DNA fragmentation and proteolysis, thus culminating in its death. Caspases have a central role in mediating the initiation and propagation of programmed cell death.[1] To date, 14 mammalian caspases have been identified, and caspases involved in apoptosis can be broadly divided into initiator or effector caspases. Each caspase remains in an inactive procaspase form in the normal cell, and upon apoptotic stimuli becomes activated and cleaves its cellular substrates by binding to a small peptide sequence.

As the dysregulation of apoptosis contributes to the development and progression of various diseases including cancer, neurodegenerative disorders, and chronic heart failure, the ability to noninvasively image caspase activation would provide an opportunity to evaluate therapeutic interventions longitudinally in living animals using various disease models. In oncology, for example, the majority of cytotoxic chemotherapeutic agents that induce apoptosis and defects in the apoptotic cascade are known to contribute to drug resistance and ultimately may lead to treatment failure.[2–4] In neuroscience, evidence suggests that reactivation of programmed cell death in dopaminergic neurons of the substantia nigra pars compacta in adulthood may contribute to the onset of Parkinson's disease.[5] Furthermore, many studies have reported extensive neuronal and glial apoptosis after injury to the central nervous system.[6] Apoptosis is also an important process fundamental to many diseases of the cardiovascular system, including chronic heart failure, atherosclerotic vascular disease, and myocardial ischemia and reperfusion injury.[7] Therefore, development of imaging probes targeting cells undergoing apoptosis may allow evaluation of therapeutic efficacy in a wide range of preclinical applications.

Recently, there has been a considerable increase in the availability of new imaging technologies to noninvasively detect biological processes in small animal models.[8–10] One such modality, optical imaging, comprises using bioluminescent and fluorescent reporters or probes and has evolved to enable observation of disease burden and progression in various therapeutic models, as well as to facilitate rapid monitoring of molecular events occurring within cells.[11,12] Several recent reports have described the development of fluorescent and/or bioluminescent reporter constructs that

[1]Global Pharmaceutical Research and Development, Abbott Laboratories, Abbott Park, IL, USA and [2]Promega Biosciences Inc., San Luis Obispo, CA, USA
*Corresponding author: J Hickson, Department R4N2, Bldg AP3, Abbott Laboratories, 100 Abbott Park Road, Abbott Park, IL 60064, USA.
Tel: +1 84 7937 0141; Fax: +1 84 7938 4777; E-mail: jonathan.hickson@abbott.com
Keywords: cancer; drug development; general physiology
Abbreviations: BLI, bioluminescent imaging; i.p., intraperitoneal; MRI, magnetic resonance imaging; PET, positron emission tomography; ROI, region-of-interest; SCID, severe combined immunodeficient; SPECT, single-photon emission computed tomography
Received 15.5.09; revised 05.11.09; accepted 18.11.09; Edited by B Zhivotovsky; published online 08.1.10

specifically allow monitoring of caspase activation *in vivo*. These molecular imaging studies have mainly focused on generating cells that express a modified reporter protein, commonly a fusion protein or a split luciferase protein complementation strategy[13–15] that takes advantage of the specificity of caspases to cleave exclusively after aspartic acid residues and, in particular, the DEVD (aspartic acid–glutamic acid–valine–aspartic acid) tetrapeptide sequence, which is optimal for apoptotic effector caspases-3 and -7.[16,17] In these models, light production is silenced unless the cell is undergoing apoptosis, at which time activated caspase liberates the reporter.

In this study, we adopt an alternate approach by using intact firefly luciferase and a modified firefly luciferase substrate, Z-DEVD-aminoluciferin. This substrate has been previously characterized and is currently widely used as an *in vitro* reporter for apoptosis.[18–20] However, experiments to date have failed to transition this probe *in vivo* without acute toxicity to the animal.[21] Using chemical material purified for *in vivo* use, we report a successful formulation of Z-DEVD-aminoluciferin that is well tolerated *in vivo* after multiple doses and enables quantification of apoptosis noninvasively in two oncology models. In addition, use of this probe enabled an earlier determination of drug efficacy than using traditional methods. Importantly, because this apoptosis probe requires no modification of existing firefly luciferase-expressing cell lines or transgenic animals, it should facilitate rapid evaluation of preclinical efficacy of experimental therapeutic agents in various disease states.

Results

***In vitro* bioluminescent imaging of docetaxel-induced apoptosis.** Z-DEVD-aminoluciferin, a proluminescent caspase-3/7 substrate, has been successfully used for *in vitro* assessment of caspase-3 or caspase-7 activity.[18–20] Specific cleavage of the DEVD peptide by caspase-3/7 liberates free aminoluciferin, which is consumed by the luciferase, generating a luminescent signal that is proportional to activity. Docetaxel is a microtubule-disruptive apoptotic agent commonly used as chemotherapy medication to treat various cancer indications, and has previously been shown to be a potent activator of caspase-3/7 in human mammary (MDA-MB-231) and ovarian (SKOV3) adenocarcinoma cell lines.[22–24] To image docetaxel-induced apoptosis *in vitro*, 150 μM of Z-DEVD-aminoluciferin was added to luciferase-expressing derivatives of these cell lines treated with a range (1–4000 nM) of docetaxel concentrations for 48 h. Luminescent images were acquired using a Xenogen IVIS Spectrum imaging system (Caliper Life Sciences, Hopkinton, MA, USA), and activation of caspase-3/7 was quantified. Representative images for MDA-MB-231-luc-LN cells are shown in Figure 1a. Increasing luminescent signal corresponded to higher docetaxel concentrations, reflecting elevated caspase activation. As a measure of cell viability, 150 μM of aminoluciferin was added to a parallel set of cells. Luminescent signal decreased with increasing docetaxel concentrations, reflecting increasing apoptosis and cell death. When the luminescent signal in each well was quantified, both aminoluciferin and Z-DEVD-aminoluciferin yielded similar cellular EC_{50} values (2.48 and 2.02 nM, respectively; Figure 1b), which is consistent with previously reported values.[25] Probe specificity was demonstrated by treating MDA-MB-231-luc-LN cells with doxorubicin, which induced cell death in this cell line through a caspase-3-independent mechanism, and therefore generated no bioluminescent signal after addition of the Z-DEVD-aminoluciferin substrate (Supplementary Figure 1).

Pharmacokinetics of Z-DEVD-aminoluciferin. Unlike the DEVD peptide or aminoluciferin, both of which are freely soluble in water, the Z-DEVD-aminoluciferin construct demonstrated a strong tendency toward aggregation at high concentrations required for *in vivo* imaging which could

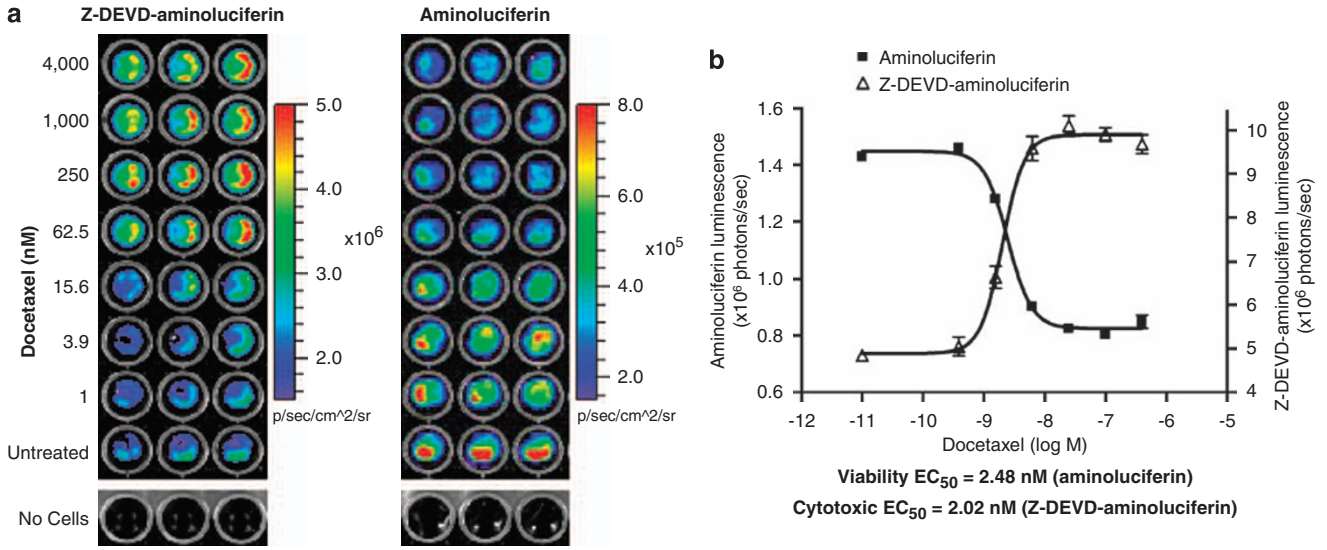

Figure 1 *In vitro* bioluminescent imaging of docetaxel-induced apoptosis. (**a**) MDA-MB-231-luc-LN cells were treated with various concentrations of docetaxel for 48 h. A total of 150 μM of Z-DEVD-aminoluciferin or aminoluciferin was then added to determine cellular apoptosis or proliferation, respectively. (**b**) Luciferase activity in each well was quantified, with mean values ± S.E.M. ($n = 3$) plotted and EC_{50} values determined

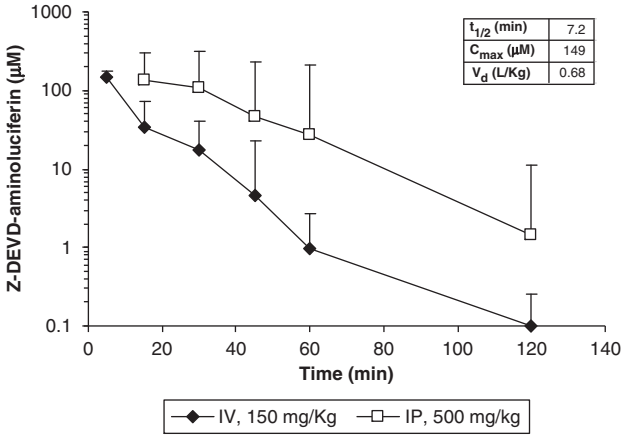

Figure 2 *In vivo* pharmacokinetics of Z-DEVD-aminoluciferin. Plasma concentrations after administration of 150 mg/kg intravenously (black diamonds) or 500 mg/kg intraperitoneally (open squares) in female SCID mice. Mean ± S.E.M. ($n=3$) is shown. Inset contains calculated half-life, C_{max}, and V_d for Z-DEVD-aminoluciferin

only be forestalled by DMSO. In the presence of 5% DMSO, a mixture of polyethylene glycol 400 (PEG400) and polysorbate 80 could achieve solubility at high concentrations. Female severe combined immunodeficient (SCID) mice were dosed with Z-DEVD-aminoluciferin intravenously (150 mg/kg) or intraperitoneally (i.p., 500 mg/kg), and blood was harvested for more than 2 h for pharmacokinetic analysis ($n=3$ mice per time point). Z-DEVD-aminoluciferin was rapidly absorbed from the peritoneum, with a C_{max} value of 149 μM, and was rapidly cleared from plasma ($t_{1/2}=7.2$ min) (Figure 2). Furthermore, Z-DEVD-aminoluciferin had a volume of distribution (V_d) equating to total body water, suggesting that the probe freely crosses cell membranes. Importantly, no toxicity was observed after multiple daily doses of Z-DEVD-aminoluciferin at 500 mg/kg. All these are ideal characteristics for an *in vivo* imaging probe.

***In vivo* bioluminescent imaging of docetaxel-induced apoptosis.** To evaluate Z-DEVD-aminoluciferin *in vivo*, SKOV3-luc cells were inoculated subcutaneously into the flank of female SCID mice and tumors were allowed to establish. Animals were size matched into two groups ($n=3$ per group) and bioluminescent images were acquired after i.p. injection of mice with 150 mg/kg of luciferin. Mice were then treated intravenously with 60 mg/kg of docetaxel or vehicle. At 24, 48, and 72 h after treatment, animals were injected daily with 500 mg/kg Z-DEVD-aminoluciferin i.p., and bioluminescent images were acquired every minute for 1 h. A parallel set of animals was treated identically and tumors were collected for immunohistochemical analysis.

In vivo luciferase activity was quantified using region-of-interest (ROI) analysis of the bioluminescent images acquired before treatment with luciferin and after treatment using Z-DEVD-aminoluciferin. Representative images of both treated and untreated groups at each time point are shown in Figure 3a. As expected, after size matching, the pretreatment images using luciferin demonstrate equivalent amount of luminescent signal originating from the tumor in both groups. Data acquired from images using the Z-DEVD-aminoluciferin substrate indicate that significantly more light was detected at 48 and 72 h ($P<0.05$) in the docetaxel-treated group than in the vehicle-treated group (Figure 3b). Similar to *in vivo* luciferin kinetics, 10–20 min post Z-DEVD-aminoluciferin injection yielded the highest fold increase, ranging from two to threefold, and provided proof-of-concept validation for the use of this probe to monitor apoptosis *in vivo*. As shown in Figures 3c and d, docetaxel induced activation of caspase-3 in SKOV3-luc tumors as early as 24 h after treatment, which remained activated at 48 and 72 h, compared with vehicle-treated tumors. Representative H&E and luciferase immunohistochemistry staining is also shown, confirming luciferase expression in tumor cells.

To confirm these results in an additional model with an expanded number of animals, MDA-MB-231-luc-LN cells were inoculated subcutaneously into the flank of female SCID mice and tumors were allowed to establish. After size matching on the basis of tumor volume, mice ($n=8$ per group) were treated and imaged in a similar manner as described above, with additional tumors harvested for immunohistochemical analysis. ROI analysis was completed on the bioluminescent images before treatment using luciferin and after treatment using Z-DEVD-aminoluciferin. Representative images of both treated and untreated groups at each time point are shown in Figure 4a. Similar amounts of signal were detected in all mice before treatment using the luciferin substrate. However, daily administration of the Z-DEVD-aminoluciferin substrate resulted in significantly more light detected at 24 ($P<0.05$), 48 ($P<0.01$), and 72 h ($P<0.01$) in the docetaxel-treated group compared with the vehicle-treated group (Figure 4b). Similar to the pilot study described above, 10–20 min post Z-DEVD-aminoluciferin injection again yielded the highest fold increase in bioluminescent signal. As shown in Figures 4c and d, docetaxel induced activation of caspase-3 in these tumors by 24 h after treatment, which increased at 48 and 72 h, compared with vehicle-treated tumors. Representative H&E and luciferase IHC staining is also shown, confirming luciferase expression in this tumor type. Taken together, these studies confirm that Z-DEVD-aminoluciferin can be used as a sensitive noninvasive bioluminescent *in vivo* apoptosis probe.

Earlier detection of therapeutic efficacy *in vivo* using Z-DEVD-aminoluciferin. Of critical importance to drug discovery and development is the need to rapidly assess therapeutic efficacy *in vivo*. Tumor volume was measured for MDA-MB-231-luc-LN tumor-bearing mice represented in Figure 4, until each group reached an end point of $\sim$2500 mm^3 (Figure 5a). Whereas significant differences were detected as early as 24 h after treatment by molecular imaging using Z-DEVD-aminoluciferin, caliper measurements were unable to detect a difference for 4–5 additional days (Figure 5b). Although the use of this probe significantly shortened the time necessary to determine treatment efficacy in subcutaneous MDA-MB-231-luc-LN tumors, it could provide an even more dramatic improvement in indicating antitumor efficacy in models that are relatively slow growing, as well as provide a method for determining drug efficacy in orthotopic, ectopic, or systemic

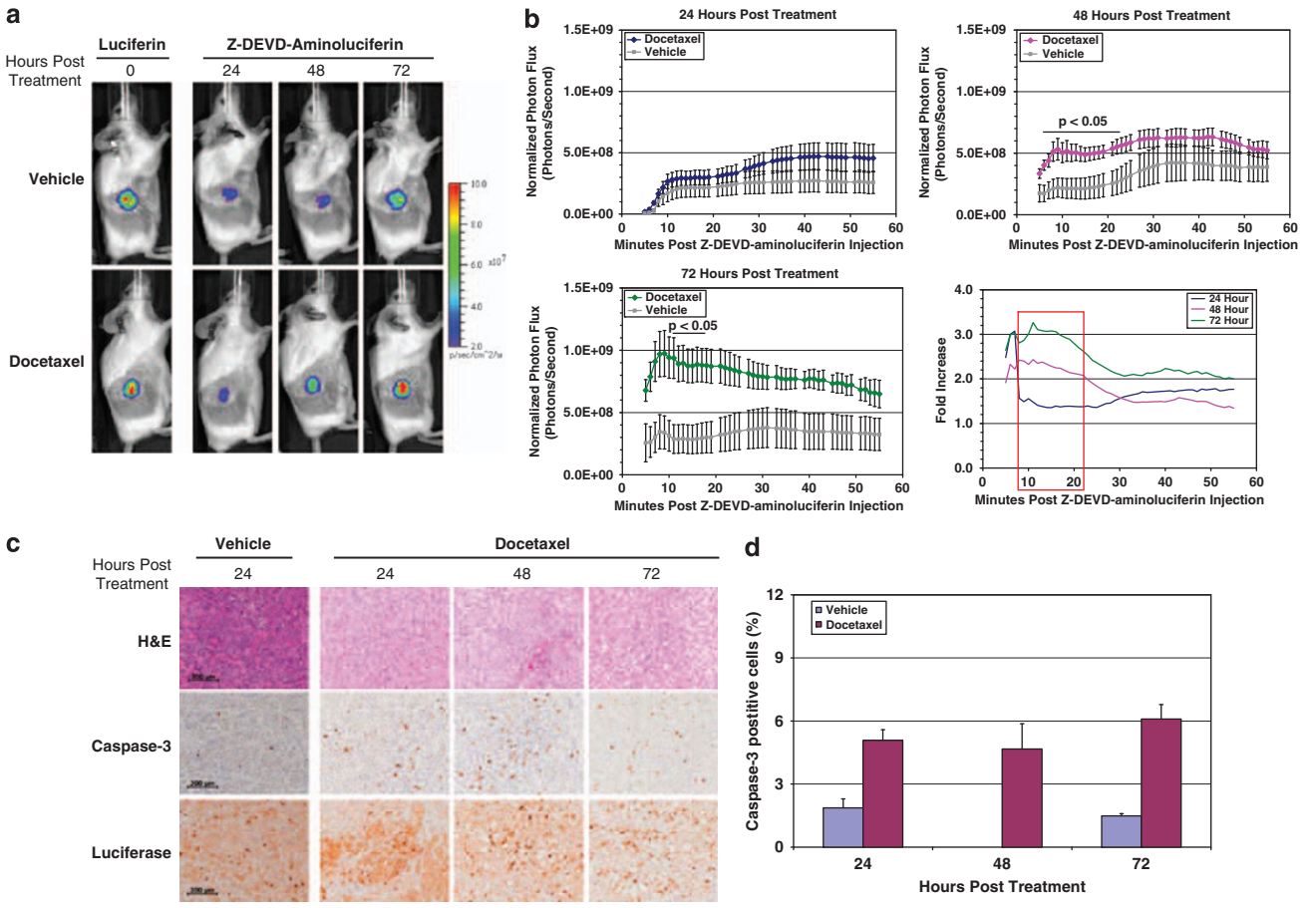

Figure 3 Longitudinal bioluminescent imaging of caspase activation in SKOV3-luc tumors using Z-DEVD-aminoluciferin. (**a**) Representative bioluminescent images of vehicle- and docetaxel-treated mice at each time point 15 min after injection of substrate. (**b**) Bioluminescent images were acquired every minute for 1 h after substrate injection and *in vivo* luciferase activity was quantified. Mean ± S.E.M. ($n = 3$) for each group at 24, 48, and 72 h after treatment is shown. When normalized to vehicle, a three-fold higher signal was observed in mice 72 h after docetaxel treatment. Red box indicates optimal time post Z-DEVD-aminoluciferin injection to image. (**c**, **d**) Confirmation of docetaxel-induced apoptosis in SKOV3-luc tumors. (Panel c) Immunohistochemistry for cleaved caspase-3 demonstrated induction of caspase-3 as early as 24 h after treatment, which remained activated at 48 and 72 h, compared with vehicle-treated tumors. Representative H&E and luciferase immunohistochemistry staining is also shown, confirming luciferase expression in the tumor cells. Scale bars, 200 μm. (Panel d) Quantification of activated caspase-3-positive cells of entire sections of the tumor, excluding necrotic regions

models in which longitudinal measurements of tumor burden are not possible. Taken together, these data show that *in vivo* imaging of apoptosis using Z-DEVD-aminoluciferin could provide a sensitive and rapid method for early detection of drug efficacy.

Discussion

In this study, we report the ability to noninvasively detect caspase-3 activation in response to chemotherapy in two preclinical oncology models. We demonstrate that the modified luciferase substrate Z-DEVD-aminoluciferin can be formulated and well tolerated as an *in vivo* agent. The two- to three-fold induction of bioluminescent signal at 48 and 72 h after docetaxel treatment in both models is consistent with the two- to four-fold increase in activated caspase-3 as determined by immunohistochemistry. The use of agents that elicit a more robust activation of apoptosis (e.g., TRAIL) in appropriate *in vivo* model(s) could potentially yield an even larger window of utility, although caspase activation to the degree observed in this study after docetaxel treatment may be more commonplace. Finally, we show that the use of this optical imaging probe can significantly decrease the time required for determining preclinical drug efficacy compared with using traditional methods. To the best of our knowledge, this is the first *in vivo* report using a bioluminescent apoptosis substrate with long-term animal survival and therapeutic efficacy data.

Recently, there have been several published reports using elegant luminescent reporter systems in preclinical models to detect apoptosis *in vivo* by optical imaging. One approach has been to create reporter constructs in which luminescent activity is silenced by fusion to other peptide sequences. In one example, two estrogen-regulatory domains were linked on both the amino- and carboxy-terminal end of luciferase with a DEVD cleavage site.[13,14] Similarly, a multimodality imaging reporter was also recently described to be composed of fluorescent, bioluminescent, and positron emission

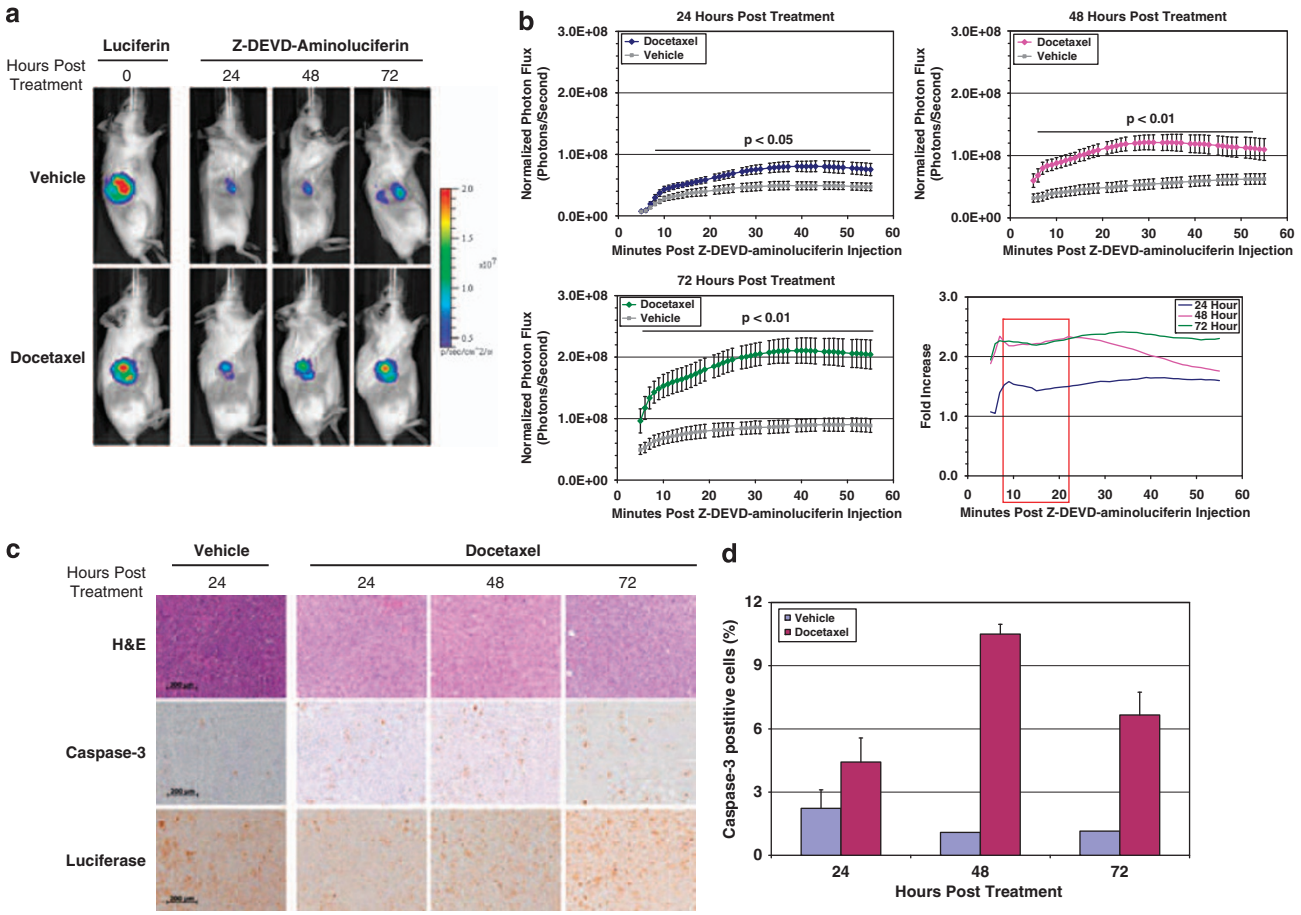

Figure 4 Longitudinal bioluminescent imaging of caspase activation in MDA-MB-231-luc-LN tumors using Z-DEVD-aminoluciferin. (**a**) Representative bioluminescent images of vehicle- and docetaxel-treated mice at each time point 15 min after injection of substrate. (**b**) Bioluminescent images were acquired every minute for 1 h after substrate injection and *in vivo* luciferase activity was quantified. Mean ± S.E.M. ($n = 8$) for each group at 24, 48, and 72 h after treatment is shown. Significantly more light was detected in the docetaxel-treated group at all time points compared with the vehicle-treated group. Red box indicates optimal time post Z-DEVD-aminoluciferin injection to image. (**c**, **d**) Confirmation of docetaxel-induced apoptosis in MDA-MB-231-luc-LN tumors. (Panel c) Immunohistochemistry for cleaved caspase-3 demonstrated induction of caspase-3 as early as 24 h after treatment, which remained activated at 48 and 72 h, compared with vehicle-treated tumors. Representative H&E and luciferase immunohistochemistry staining is also shown, confirming luciferase expression in the tumor cells. Scale bars, 200 μm. (Panel d) Quantification of activated caspase-3-positive cells of entire sections of the tumor, excluding necrotic regions

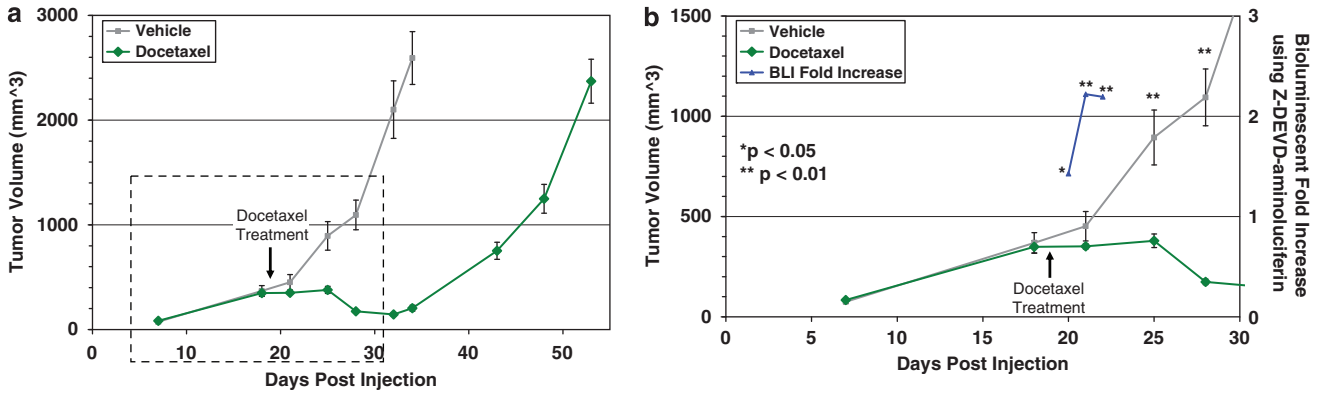

Figure 5 Enhanced detection of *in vivo* therapeutic efficacy after docetaxel treatment using Z-DEVD-aminoluciferin. (**a**) Tumor volume of female SCID mice bearing subcutaneous MDA-MB-231-luc-LN tumors treated with a single dose of vehicle or docetaxel (60 mg/kg) 19 days after inoculation. Mean ± S.E.M. ($n = 8$) is shown. (**b**) An expanded view of the first 30 days after inoculation highlights that significant differences between treatment groups were detected earlier using bioluminescent imaging (days 20–22) compared with caliper measurements (day 25)

tomography (PET) reporters, separated by DEVD linkers.[26] In both models, under apoptotic conditions, the reporter domains are liberated allowing for light production. Other methods for monitoring apoptosis *in vivo* have used a reporter protein complementation strategy, such as a split luciferase model. In this system, the amino- and carboxy-terminal domains of luciferase are fused to strongly interacting peptides that are linked by an enzyme-specific sequence.[27–34] Cleavage of the linker permits the interacting peptides to associate, allowing reconstitution of luciferase activity. Coppola *et al.*[15] described development of a split firefly luciferase reporter strategy in which DEVD is used as the intervening cleavage sequence and also reported the ability to detect activation of apoptosis *in vivo* after treatment with chemotherapeutic agents. However, a limitation to these strategies is the relatively large molecular size of the reporters that need to be transfected or transduced into the host cell. In addition, the intensity of luminescent signal can be diminished because of insufficient digestion of the DEVD sequence during apoptosis. Furthermore, as is the case with most protein complementation assays, activity of the combined luciferase is often lower than that of the intact reporter. Another important advantage of using a modified luciferin substrate, such as Z-DEVD-aminoluciferin described in this study, is that any existing cell line or transgenic mouse with firefly luciferase expression can be used immediately without extensive rederivation and characterization of model systems.

Similar strategies for detecting apoptosis *in vivo* have been adopted using fluorescent reporters. Bardet *et al.*[35] described the design of a reporter system that involved two fused fluorescent proteins that were linked to a caspase-sensitive site. Upon cleavage, the two moieties became differentially localized because of subcellular localization signals allowing identification of those cells undergoing cell death. Other strategies have focused on using membrane-permeant fluorescent-labeled inhibitors of caspases (FLICA) probe technology.[36] FLICA probes are high-affinity ligands that irreversibly covalently bind to the cysteine at the active center of caspase.[37,38] Another approach has been to develop fluorescent probes that are capable of selectively recognizing and binding to apoptotic cell membrane features. One such compound, FI-ApoSense, has successfully been used preclinically for imaging apoptosis-induced cells and tissues in myocardial, cerebral, and renal ischemia models, as well as in oncology models.[39–43] It is noteworthy that a radiolabeled analog is currently being evaluated as a PET probe in a phase II study to assess the response of metastatic brain tumors to radiotherapy, highlighting how optical imaging probes can prototype clinical PET, single-photon emission computed tomography (SPECT) or magnetic resonance imaging (MRI) probes.[44] Although these and other fluorescent strategies have proved useful in reporting caspase activation *in vitro* and with tissues *ex vivo*, they are yet to be fully validated as useful tools for longitudinal *in vivo* imaging of apoptosis. Furthermore, an intrinsic limitation to any fluorescent probe *in vivo*, compared with a bioluminescent reporter, is the lower signal-to-noise ratio due in part to the high degree of autofluorescence and low level of tissue penetrance at most wavelengths. As Z-DEVD-aminoluciferin is a bioluminescent reporter, it does not face many of these same challenges.

Although the molecular imaging approach outlined in this study using a bioluminescent probe cannot be directly translated into the clinic, it does have the potential to serve as an important tool for preclinical drug discovery. As we demonstrated, the Z-DEVD-aminoluciferin substrate enabled noninvasive observation of the apoptotic affects of chemotherapy several days before they could be detected through traditional methods. A large majority of the chemotherapeutic agents currently available or under development exert their effect by inducing cellular pathways that lead to programmed cell death. Consequently, this bioluminescent imaging probe has the possibility to be useful to a wide range of therapeutic applications within cancer drug discovery and development. In addition, *in vivo* optical imaging is uniquely suited for high-throughput evaluation of candidate drugs because of the ease of operation, short acquisition times, and simultaneous measurement of multiple animals as compared with the significantly longer image acquisition time of a single animal with preclinical PET, SPECT, or MRI. Finally, although our initial approach used two cancer models, caspase activation is of critical importance in many other fields. As mentioned above, cellular apoptosis not only has an essential role in normal physiology and development but is also instrumental in a number of disorders, including Parkinson's, Alzheimer's, cerebral ischemia, and many cardiovascular diseases.[5–7] Therefore, this probe may also have utility in applications across numerous therapeutic targets and research disciplines through the usage of luciferase-expressing cell lines or transgenic animal models specific to these disease states.

Materials and Methods

Cell culture. SKOV3-luc-D3 and MDA-MB-231-luc-D3H2LN were purchased from Caliper Life Sciences (Hopkinton, MA, USA). These cell lines were clonally selected after stable transfection with the pGL3 (Promega, Madison, WI, USA) luciferase and were previously characterized.[45,46] We cultured SKOV3-luc cells in McCoy's 5A with 10% fetal bovine serum (FBS), 2 mM glutamine, and 0.1 mM nonessential amino acids, whereas MDA-MB-231-luc-LN cells were cultured in MEM with 10% FBS, 2 mM glutamine, 0.1 mM nonessential amino acids, and 1 mM sodium pyruvate (all from Invitrogen, Carlsbad, CA, USA).

***In vitro* bioluminescent imaging.** We treated cells grown in 96-well plates (1×10^4 SKOV3-luc or MDA-MB-231-luc-LN cells per well) with 1–4000 nM docetaxel. After a 48-h incubation period, we added either 150 μM of aminoluciferin or Z-DEVD-aminoluciferin to each well and measured luciferase activity using a Xenogen IVIS Spectrum imaging system. Luminescent signal (photons per second) for each well was measured and plotted as average values (experiments conducted in duplicate).

***In vivo* xenografts.** We inoculated female SCID mice (Charles River Laboratories, Wilmington, MA, USA) with 1×10^6 cells subcutaneously in the right flank in a 50 : 50 mixture of cells in growth medium and Matrigel (BD Biosciences). Tumors were allowed to establish to an approximate volume of 250 mm^3, as determined by caliper measurement ($V = L \times W^2/2$). Animals were size matched into treatment groups and were dosed i.p. once with 60 mg/kg of docetaxel or vehicle. All animal studies were conducted in accordance with the guidelines established by the internal IACUC (Institutional Animal Care and Use Committee) of Abbott Laboratories (Abbott Park, IL, USA).

Formulation and delivery of luciferin substrates. Z-DEVD-aminoluciferin (VivoGlo Caspase-3/7 Substrate, Promega) was weighed into glass vials and partially dissolved in a mixture of 75% PEG400, 12.5% polysorbate 80, 12.5% DMSO and vortexed to form a slurry. Slurry was diluted 2.5-fold with 5% dextrose in water (D5W), while vortexing to prepare a final formulation consisting of 5% DMSO, 5% polysorbate 80, 30% PEG400, 60% D5W. Z-DEVD-aminoluciferin, at concentrations of up to 62.5 mg/ml, remained in solution for approximately 2–3 h

before aggregating. Luciferin was dissolved in PBS at a concentration of 15 mg/ml. We administered Z-DEVD-aminoluciferin and luciferin i.p. at 500 and 150 mg/kg, respectively.

Pharmacokinetic analysis. After Z-DEVD-aminoluciferin administration as described in this study, we collected plasma samples by intracardiac bleeding from three animals at each time point. Plasma proteins were precipitated with two volumes of acidified methanol, removed by centrifugation, and the supernatants were stored at –20 °C until analysis by liquid chromatography-mass spectrometry. Plasma extracts were injected directly on a C18-reversed phase column (YMC-5μ, Waters Corporation, Milford, MA, USA) and eluted using a gradient (LC-20 HPLC system, Shimadzu, Kyoto, Japan) from 10 to 90% acetonitrile with 0.1% acetic acid as the aqueous phase at a flow rate of 0.4 ml/min. External standards were prepared on the day of the study and concentrations were determined from the external calibration curve. Pharmacokinetic parameters were calculated using the WinNonlin software (Pharsight, St Louis, MO, USA). Mass spectrometer analysis was performed using an LXQ ion trap (Thermo Electron, Waltham, MA, USA) equipped with ESI and XCalibur software.

***In vivo* bioluminescent imaging.** After i.p. injection of luciferin or Z-DEVD-aminoluciferin, we anesthetized the animals (2% isoflurane) and acquired images continuously for 1 h using an IVIS Spectrum. We measured luciferase activity as photons per second for designated regions of interest at 24, 48, and 72 h after treatment.

Immunohistochemical analysis. We fixed tumors in neutral-buffered formalin for immunohistochemical staining for activated caspase-3 (rabbit antiactive caspase-3 at 1 : 400, BD Pharmingen, San Jose, CA, USA) and luciferase (goat antiluciferase at 1 : 1000, Promega). For quantification of activated caspase-3 staining, we used Spectum Plus (Aperio, Vista, CA, USA) color deconvolution software to analyze mosaic images acquired using a Zeiss Axiovision (Zeiss, Oberkochen, Germany) of entire sections of the tumor, excluding necrotic regions.

Statistical analysis. We used two-tailed, unpaired Student's *t*-test and considered $P < 0.05$ significant.

Conflict of interest

The authors declare no conflict of interest.

Acknowledgements. We thank Martha O'Brien, Alex Shoemaker, and Erwin Boghaert for thoughtful their discussions and manuscript proofreading. We also thank Joann Palma for her guidance on immunohistochemical techniques and analysis.

1. Grutter MG. Caspases: key players in programmed cell death. *Curr Opin Struct Biol* 2000; **10**: 649–655.
2. Haq R, Zanke B. Inhibition of apoptotic signaling pathways in cancer cells as a mechanism of chemotherapy resistance. *Cancer Metastasis Rev* 1998; **17**: 233–239.
3. Reed JC. Dysregulation of apoptosis in cancer. *J Clin Oncol* 1999; **17**: 2941–2953.
4. Kaufmann SH, Vaux DL. Alterations in the apoptotic machinery and their potential role in anticancer drug resistance. *Oncogene* 2003; **22**: 7414–7430.
5. Perier C, , Bové J, Wu DC, Dehay B, Choi DK, Jackson-Lewis V *et al.* Two molecular pathways initiate mitochondria-dependent dopaminergic neurodegeneration in experimental Parkinson's disease. *Proc Natl Acad Sci USA* 2007; **104**: 8161–8166.
6. Springer JE. Apoptotic cell death following traumatic injury to the central nervous system. *J Biochem Mol Biol* 2002; **35**: 94–105.
7. Korngold EC, Jaffer FA, Weissleder R, Sosnovik DE. Noninvasive imaging of apoptosis in cardiovascular disease. *Heart Fail Rev* 2008; **13**: 163–173.
8. Pirko I, Fricke ST, Johnson AJ, Rodriguez M, Macura SI. Magnetic resonance imaging, microscopy, and spectroscopy of the central nervous system in experimental animals. *NeuroRx* 2005; **2**: 250–264.
9. Brindle K. New approaches for imaging tumour responses to treatment. *Nat Rev Cancer* 2008; **8**: 94–107.
10. Bengel FM. Noninvasive imaging of cardiac gene expression and its future implications for molecular therapy. *Mol Imaging Biol* 2005; **7**: 22–29.
11. Sahai E. Illuminating the metastatic process. *Nat Rev Cancer* 2007; **7**: 737–749.
12. Weissleder R, Pittet MJ. Imaging in the era of molecular oncology. *Nature* 2008; **452**: 580–589.
13. Laxman B, , Hall DE, Bhojani MS, Hamstra DA, Chenevert TL, Ross BD *et al.* Noninvasive real-time imaging of apoptosis. *Proc Natl Acad Sci USA* 2002; **99**: 16551–16555.
14. Lee KC, , Hamstra DA, Bhojani MS, Khan AP, Ross BD, Rehemtulla A. Noninvasive molecular imaging sheds light on the synergy between 5-fluorouracil and TRAIL/Apo2 L for cancer therapy. *Clin Cancer Res* 2007; **13**: 1839–1846.
15. Coppola JM, Ross BD, Rehemtulla A. Noninvasive imaging of apoptosis and its application in cancer therapeutics. *Clin Cancer Res* 2008; **14**: 2492–2501.
16. Fischer U, Janicke RU, Schulze-Osthoff K. Many cuts to ruin: a comprehensive update of caspase substrates. *Cell Death Differ* 2003; **10**: 76–100.
17. Timmer JC, Salvesen GS. Caspase substrates. *Cell Death Differ* 2007; **14**: 66–72.
18. O'Brien MA, , Daily WJ, Hesselberth PE, Moravec RA, Scurria MA, Klaubert DH *et al.* Homogeneous, bioluminescent protease assays: caspase-3 as a model. *J Biomol Screen* 2005; **10**: 137–148.
19. Liu JJ, Wang W, Dicker DT, El-Deiry WS. Bioluminescent imaging of TRAIL-induced apoptosis through detection of caspase activation following cleavage of DEVD-aminoluciferin. *Cancer Biol Ther* 2005; **4**: 885–892.
20. Birdsey GM, , Dryden NH, Amsellem V, Gebhardt F, Sahnan K, Haskard DO *et al.* Transcription factor Erg regulates angiogenesis and endothelial apoptosis through VE-cadherin. *Blood* 2008; **111**: 3498–3506.
21. Shah K, Tung CH, Breakefield XO, Weissleder R. In vivo imaging of S-TRAIL-mediated tumor regression and apoptosis. *Mol Ther* 2005; **11**: 926–931.
22. Yacoub A, , Han SI, Caron R, Gilfor D, Mooberry S, Grant S *et al.* Sequence dependent exposure of mammary carcinoma cells to Taxotere and the MEK1/2 inhibitor U0126 causes enhanced cell killing in vitro. *Cancer Biol Ther* 2003; **2**: 670–676.
23. Yacoub A, , Gilfor D, Hawkins W, Park MA, Hanna D, Hagan MP *et al.* MEK1/2 inhibition promotes Taxotere lethality in mammary tumors in vivo. *Cancer Biol Ther* 2006; **5**: 1332–1339.
24. Halder J, , Landen Jr CN, Lutgendorf SK, Li Y, Jennings NB, Fan D *et al.* Focal adhesion kinase silencing augments docetaxel-mediated apoptosis in ovarian cancer cells. *Clin Cancer Res* 2005; **11**: 8829–8836.
25. Distefano M, , Scambia G, Ferlini C, Gaggini C, De Vincenzo R, Riva A *et al.* Anti-proliferative activity of a new class of taxanes (14beta-hydroxy-10-deacetylbaccatin III derivatives) on multidrug-resistance-positive human cancer cells. *Int J Cancer* 1997; **72**: 844–850.
26. Ray P, De A, Patel M, Gambhir SS. Monitoring caspase-3 activation with a multimodality imaging sensor in living subjects. *Clin Cancer Res* 2008; **14**: 5801–5809.
27. Ozawa T, Kaihara A, Sato M, Tachihara K, Umezawa Y. Split luciferase as an optical probe for detecting protein-protein interactions in mammalian cells based on protein splicing. *Anal Chem* 2001; **73**: 2516–2521.
28. Kaihara A, Kawai Y, Sato M, Ozawa T, Umezawa Y. Locating a protein-protein interaction in living cells via split Renilla luciferase complementation. *Anal Chem* 2003; **75**: 4176–4181.
29. Paulmurugan R, Gambhir SS. Monitoring protein-protein interactions using split synthetic renilla luciferase protein-fragment-assisted complementation. *Anal Chem* 2003; **75**: 1584–1589.
30. Kim SB, Otani Y, Umezawa Y, Tao H. Bioluminescent indicator for determining protein-protein interactions using intramolecular complementation of split click beetle luciferase. *Anal Chem* 2007; **79**: 4820–4826.
31. Paulmurugan R, Umezawa Y, Gambhir SS. Noninvasive imaging of protein-protein interactions in living subjects by using reporter protein complementation and reconstitution strategies. *Proc Natl Acad Sci USA* 2002; **99**: 15608–15613.
32. Paulmurugan R, Gambhir SS. Novel fusion protein approach for efficient high-throughput screening of small molecule-mediating protein-protein interactions in cells and living animals. *Cancer Res* 2005; **65**: 7413–7420.
33. Paulmurugan R, Gambhir SS. An intramolecular folding sensor for imaging estrogen receptor-ligand interactions. *Proc Natl Acad Sci USA* 2006; **103**: 15883–15888.
34. Kim SB, Ozawa T, Watanabe S, Umezawa Y. High-throughput sensing and noninvasive imaging of protein nuclear transport by using reconstitution of split Renilla luciferase. *Proc Natl Acad Sci USA* 2004; **101**: 11542–11547.
35. Bardet PL, , Kolahgar G, Mynett A, Miguel-Aliaga I, Briscoe J, Meier P *et al.* A fluorescent reporter of caspase activity for live imaging. *Proc Natl Acad Sci USA* 2008; **105**: 13901–13905.
36. Lee BW, Olin MR, Johnson GL, Griffin RJ. In vitro and in vivo apoptosis detection using membrane permeant fluorescent-labeled inhibitors of caspases. *Methods Mol Biol* 2008; **414**: 109–135.
37. Smolewski P, , Bedner E, Du L, Hsieh TC, Wu JM, Phelps DJ *et al.* Detection of caspases activation by fluorochrome-labeled inhibitors: Multiparameter analysis by laser scanning cytometry. *Cytometry* 2001; **44**: 73–82.
38. Bedner E, Smolewski P, Amstad P, Darzynkiewicz Z. Activation of caspases measured in situ by binding of fluorochrome-labeled inhibitors of caspases (FLICA): correlation with DNA fragmentation. *Exp Cell Res* 2000; **259**: 308–313.
39. Dumont EA, , Reutelingsperger CP, Smits JF, Daemen MJ, Doevendans PA, Wellens HJ. Real-time imaging of apoptotic cell-membrane changes at the single-cell level in the beating murine heart. *Nat Med* 2001; **7**: 1352–1355.
40. Damianovich M, , Ziv I, Heyman SN, Rosen S, Shina A, Kidron D *et al.* ApoSense: a novel technology for functional molecular imaging of cell death in models of acute renal tubular necrosis. *Eur J Nucl Med Mol Imaging* 2006; **33**: 281–291.

41. Aloya R, , Shirvan A, Grimberg H, Reshef A, Levin G, Kidron D *et al.* Molecular imaging of cell death in vivo by a novel small molecule probe. *Apoptosis* 2006; **11**: 2089–2101.
42. Reshef A, , Shirvan A, Grimberg H, Levin G, Cohen A, Mayk A *et al.* Novel molecular imaging of cell death in experimental cerebral stroke. *Brain Res* 2007; **1144**: 156–164.
43. Cohen A, , Ziv I, Aloya T, Levin G, Kidron D, Grimberg H *et al.* Monitoring of chemotherapy-induced cell death in melanoma tumors by N,N'-Didansyl-L-cystine. *Technol Cancer Res Treat* 2007; **6**: 221–234.
44. Licha K, Olbrich C. Optical imaging in drug discovery and diagnostic applications. *Adv Drug Deliv Rev* 2005; **57**: 1087–1108.
45. Jenkins DE, Hornig YS, Oei Y, Dusich J, Purchio T. Bioluminescent human breast cancer cell lines that permit rapid and sensitive in vivo detection of mammary tumors and multiple metastases in immune deficient mice. *Breast Cancer Res* 2005; **7**: R444–R454.
46. Scheffold C, Kornacker M, Scheffold YC, Contag CH, Negrin RS. Visualization of effective tumor targeting by CD8+ natural killer T cells redirected with bispecific antibody F(ab')(2)HER2xCD3. *Cancer Res* 2002; **62**: 5785–5791.

Supplementary Information accompanies the paper on Cell Death and Differentiation website (http://www.nature.com/cdd)